A noise less-sensing semi-implicit discretization of a homogeneous differentiator : principle and application

Loïc Michel, Malek Ghanes, Franck Plestan, Yannick Aoustin, Jean-Pierre Barbot

A noise less-sensing semi-implicit discretization of a homogeneous differentiator : principle and application

Loïc MICHEL, Malek GHANES, Franck PLESTAN, Yannick AOUSTIN and Jean-Pierre BARBOT

***Abstract*— Based on the projector introduced in recent Euler semi-implicit methods, the main contribution of this paper is the reduction of the effect of noise on the sliding surface of the discretized homogeneous differentiator. For that, an adaptation law according to the magnitude of the high frequency noise is proposed to modify the behavior of the projector when the discretized differentiator remains on the sliding surface. In presence of noise, the differentiator will have an asymptotic convergence but will be less-sensing noise. Otherwise, when the differentiator is not affected by noise on the sliding surface, its convergence will be in finite-time. Experimental results are shown in order to highlight the well founded of the contribution.**

I. Introduction

This paper is dedicated to the problem of reduction of the noise in the context of real-time signal differentiation using sliding mode techniques, for which interesting robustness properties are highlighted. The introduction of the implicit framework ten years ago by Acary & Brogliato [1], whose principle consists in replacing the sign function by an *implicit projector*, made a significant step towards the reduction of chattering effect while maintaining robust performances under lower sampling frequencies. Recent investigations have shown very promising results and experimental validations of some implicit based sliding mode control algorithms have been successfully performed (see e.g. [2], [3], [4], [5], [6], [7], [8], [9], [10]). Recently, the so-called implicit approach has been extended to homogeneous structures, where the authors propose a semi-implicit homogeneous observer-based control architecture [11] as well as homogeneous differentiators developed through an experimental comparative study (among some of the last published results, see [12]). In the latter, more particularly, the possibility of reducing the noise has been highlighted thanks to a semi-implicit projection with a constant parameter θ^i, this parameter improving the convergence properties of the differentiator. This approach has given encouraging results with respect to lower sampling frequencies.

In the sequel, this work proposes to investigate the dynamic adaptation of the parameter θ^i in the semi-implicit version of a very recent continuous explicit differentiator [13]. In this latter, an adaptive law drives the homogeneous exponent according to the magnitude of the measured output noise. The aim of this paper is to build an adaptive homogeneous discretized semi-implicit differentiator based on an adaptive scheme that drives the implicit projector according to the magnitude of the high frequency noise. The experimental evaluation of the proposed adaptive differentiating method is conducted on an electropneumatic set-up where the goal is to obtain the velocity and acceleration estimations from the position measurement. Since the physical characteristics of the experimental bench enormously vary over time, the physical parameters of this bench are poorly known and difficult to identify with precision. The used experimental set-up is a complete framework that has been extensively used to validate sliding based control laws [5], [12], [14], [15]; so, it is very appropriated to investigate differentiation structures.

The remainder of the present paper is organized as follows. Section II presents the experimental set-up that is composed by electropneumatic actuators. Section III reviews the implicit approaches including the homogeneous semi-implicit form that has been recently proposed in [11] and the cascaded homogeneous semi-implicit differentiation proposed in [12]. Section IV presents the proposed θ^i-projection approach whose purpose is the improvement of the robustness of the differentiation with respect to the noise. Experimental results are illustrated in Section V. Section VI gives some concluding remarks.

II. System under study: electropneumatic set-up

The experimental set-up used to evaluate the differentiators consists of two pneumatic actuators which are controlled by two servo-distributors (see Fig. 1). Each actuator is composed by two chambers denoted by P (positive) and N (negative). The position of one of these two actuators, named "Main actuator" can be controlled, whereas the second actuator, named "Perturbation actuator" and mechanically connected to the "Main" one, allows producing an external perturbation force. Under a nominal 7-bar source pressure, the maximum produced force is 2720 N; furthermore, both actuators have the same physical features: piston diameter of the pneumatic actuator is 80 mm and rod diameter 25 mm.

Remark : The system is nonlinear and is influenced by continuous perturbations generated by the perturbation actuator in Fig. 1; thereby, the focus is made on the differentiators to simultaneously overcome this perturbation

Loïc MICHEL is with École Centrale de Nantes-LS2N, UMR 6004 CNRS, Nantes, France loic.michel@ec-nantes.fr

Malek GHANES is with École Centrale de Nantes-LS2N, UMR 6004 CNRS, Nantes, France malek.ghanes@ec-nantes.fr

Franck PLESTAN is with École Centrale de Nantes-LS2N, UMR 6004 CNRS, Nantes, France franck.plestan@ec-nantes.fr

Yannick AOUSTIN is with Université de Nantes-LS2N, UMR 6004 CNRS, Nantes yannick.aoustin@univ-nantes.fr

Jean-Pierre BARBOT is with LS2N, UMR 6004 CNRS, Nantes, France barbot@ensea.fr

Manuscript 440 submitted to 2021 European Control Conference (ECC).
Received November 25, 2020.

along with the measurement noise. Moreover, the temperature of the system varies with respect to many factors (whether, operation time...) that seriously influences the state estimations.

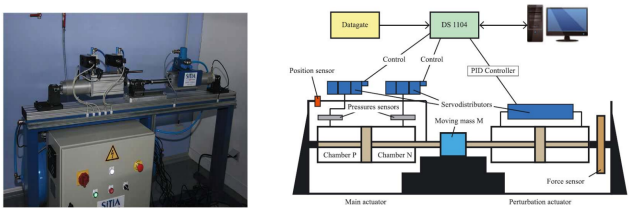

Fig. 1: Left: photography of the pneumatic setup. Right: scheme of the control architecture of the pneumatic setup (details in [14]).

A dSPACE© system allows controlling the "Main" actuator as well as monitoring the variables in real-time. Only the position is measured and the "Main" actuator is controlled using a scheme based on both linear and sliding mode approaches (see [16] [15]).

A. Model of the mechanical part

The phenomena which define the physical behavior of this experimental test-bed are complex. They are described through a model based on nonlinear and non-stationary equations including not well-defined parameters. This model can be simplified by stating hypotheses to simulate the process and with efficiency in order to predict easily its behavior and to define an efficient control as in [14].
In the sequel, given that the purpose is the differentiation of actuator position, only the mechanical part of the model is recalled; so, the pressure dynamics are viewed as external signals (for further information on pressure dynamics, see [14]).
The mathematical model of the mechanical part of the pneumatic actuator reads as:

$$\Sigma : \left\{ \begin{array}{rcl} \dot{x}_1 & = & x_2 \\ \dot{x}_2 & = & x_3 \\ \dot{x}_3 & = & d \\ y & = & x_1 + \eta \end{array} \right. \tag{1}$$

where x_1, x_2, and x_3 are respectively the position, the velocity and the acceleration of the actuator; y is the measure of x_1 with additional white noise η. The term d represents the jerk of the system such as:

$$d = \frac{1}{N}[S(\dot{p}_P - \dot{p}_N) - b_v x_3 - \dot{F}_{ext}] \tag{2}$$

where the only unknown term in (2) is the $\dot{F}_{ext}$ which can be considered as a perturbation in this model under study. Both the terms $\dot{p}_P$ and $\dot{p}_N$ are the dynamics of the pressures in both the chambers (p_P (resp. p_N) being the pressure in the chamber P (resp. N) of the actuator and are respectively function of x_1, p_P, p_N and x_2 (see details in [14]). Remark that the observability condition (see [17]) is verified for system (1).

B. Cascaded estimations

In the sequel, the semi-implicit Euler discretization technique is considered to synthesize a differentiator for system (1), whose measurements are under sampled. As the design of a third order semi-implicit differentiator would be difficult to implement, a cascaded composition of two second order homogeneous semi-implicit differentiators is considered, the first one providing sequentially, the position and the velocity, and the second one, the velocity and the acceleration of the system (1).

III. Implicit approach

A. Original Implicit

In the framework of the implicit approach [1] [3], considering a measured and noisy signal y, the corresponding discrete differentiator can be written:

$$\begin{array}{l} z_1^+ = z_1 + h\left(z_2^+ + \lambda_1 \mathcal{N}(e_1, \lambda_1)\right) \\ z_2^+ = z_2 + h\left(\lambda_2 \mathcal{N}(e_1, \lambda_1)\right) \end{array} \tag{3}$$

where the variable $\bullet^+$ corresponds to the value at instant $\bullet((k+1)h)$; e_1 is the estimation error such as $e_1 = y - z_1$; λ_1 and λ_2 are the gains of the differentiator. The projector is defined as follows:

$$\mathcal{N}(e_1, \lambda_1) := \left\{ \begin{array}{ll} \dfrac{e_1}{\lambda h} & \textbf{if} \quad e_1 < \lambda h \\ \mathrm{sgn}(e_1) & \textbf{if} \quad e_1 \geq \lambda h \end{array} \right. \tag{4}$$

B. Semi-Implicit

Homogeneous control is a more general class of finite time methods (for appropriate homogeneous degree) [18] [19] that may ensure finite-time convergence; furthermore, it is robust with respect to model uncertainties. Besides convergence issues, from the control and observation points of view, when associated to the so-called implicit projector, the main practical aspect of the homogeneity is to significantly reduce the chattering effects. A semi-implicit homogeneous version of the differentiator [11] reads as:

$$\begin{array}{l} z_1^+ = z_1 + h\left(z_2^+ + \lambda_1 |e_1|^{\alpha} \mathcal{N}_{SI}(e_1, \alpha, \lambda_1)\right) \\ z_2^+ = z_2 + h\left(\lambda_2 |e_1|^{2\,\alpha - 1} \mathcal{N}_{SI}(e_1, \alpha, \lambda_1)\right) \end{array} \tag{5}$$

where $(\lambda_1, \lambda_2) > 0$ and $\alpha \in [0, 1[$ being constant tuning parameters. The corresponding projector is defined by:

$$\mathcal{N}_{SI}(e_1, \alpha, \lambda_1) \left\{ \begin{array}{ll} \dfrac{|e_1|^{1-\alpha}}{\lambda h}\mathrm{sgn}(e_1) & \textbf{if} \quad |e_1|^{1-\alpha} < \lambda h \\ \mathrm{sgn}(e_1) & \textbf{if} \quad |e_1|^{1-\alpha} \geq \lambda h \end{array} \right. \tag{6}$$

C. Cascaded structure

In order to obtain estimations of the position x_1, the velocity x_2 and the acceleration x_3 of the pneumatic actuator, a cascaded iterative of homogeneous differentiator structure, inspired from [20], [21], [22], has been considered by the authors in [12] in order to estimate the velocity and the acceleration of the pneumatic actuator. A schematic representation is given in Fig. 2 where the term u is the

Manuscript 440 submitted to 2021 European Control Conference (ECC).
Received November 25, 2020.

control input applied to the actuator, y_{meas} is the measured position from the system (the only available measurement), and the differentiators "a" and "b" represent the cascaded nature of the two second order differentiators. The following notations are used: $y^a = y$ is the measured output, z_1^a, z_2^a are respectively the estimated position and velocity given by the first differentiator, $y^b = z_2^b$ is the output of the second differentiator, z_1^b and z_2^b are respectively the velocity and acceleration estimates by the second differentiator and $e_1^a = y^a - z_1^a = y - z_1^a$ and $e_1^b = y^b - z_1^b = z_2^a - z_1^b$ are respectively the output errors of the first and second differentiators.

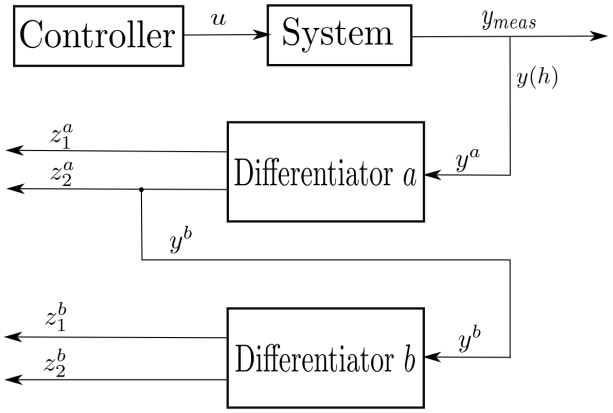

Fig. 2: Synoptic view of the proposed cascaded differentiators to estimate velocity and acceleration.

This allows a certain flexibility using different choices of homogeneous exponent α_a and α_b for the differentiators, but with the same structure. The signal measurement y_{meas} to differentiate is sampled under the sampling rate h and the proposed cascaded differentiation reads:

$$\begin{array}{l} z_1^{i+} = z_1^i + h\left(z_2^{i+} + \lambda_1^i |e_1^i|^{\alpha_i} \mathcal{N}(e_1^i, \alpha_i, \lambda_1^i)\right) \\ z_2^{i+} = z_2^i + h\left(\lambda_2^i |e_1^i|^{2\,\alpha_i - 1} \mathcal{N}(e_1^i, \alpha_i, \lambda_1^i)\right) \end{array} \tag{7}$$

where the projector $\mathcal{N}(e_1^i, \alpha_i, \lambda_1^i)$ is defined as follows:

$$\mathcal{N}(e_1^i, \alpha_i, \lambda_1^i) := \begin{cases} \dfrac{\lceil e_1^i \rfloor^{1-\alpha_i}}{\lambda_1^i h}, \text{ if } |e_1^i|^{1-\alpha_i} < \lambda_1^i h \\ \\ \mathrm{sgn}(e_1^i), \text{ if } |e_1^i|^{1-\alpha_i} \geq \lambda_1^i h \end{cases} \tag{8}$$

where $i \in \{a, b\}$ denotes the index of the considered stage "a" or "b" of the differentiation structure. As it is previously noted in the case of a cascade of two second order differentiators of the form (7), the homogeneity degree can thus be adjusted independently according to how much the output is noisy. In this work, rather than considering these homogeneity degrees as adaptive variables, the properties of the implicit projector $\mathcal{N}(e_1^i, \alpha_i, \lambda_1^i)$ are of interest and an additional parameter θ^i is introduced as described in the next section. This parameter will be dynamically adapted in order to improve the quality of the differentiation.

IV. θ^i-APPROACH FOR SEMI-IMPLICIT DIFFERENTIATOR

A. Case 1: constant θ^i

To improve the robustness with respect to the noise, a modification of the projector (8) used in the semi-implicit estimator (7) has been proposed in [12] and reads as (with $\theta^i \in [0, 1]$ and $i \in \{a, b\}$):

$$\mathcal{N}_{\theta^i}(e_1^i, \alpha_i, \lambda_1^i) := \begin{cases} \dfrac{(1-\theta^i)\lceil e_1^i \rfloor^{1-\alpha_i}}{\lambda_1^i h}, \text{ if } (1-\theta)|e_1^i|^{1-\alpha_i} < \lambda_1^i h \\ \\ \mathrm{sgn}(e_1^i), \text{ if } |e_1^i|^{1-\alpha_i} \geq \lambda_1^i h \end{cases} \tag{9}$$

with $\theta^i \in [0, \quad 1[$.
The parameter θ^i is introduced in order to mitigate the influence of noise. Basically, for $\theta^i = 0$, the previous projector equals (8), the convergence of the differentiator is finite time. When θ^i is different from zero, the convergence is only asymptotic but the differentiator is less sensible to noise. This is due to the fact that the influence of noise is multiplied by $(1 - \theta^i)$ in (9); thus, it improves the behavior of the differentiator in regard to the measurement noise.

Practically, θ^i can be chosen as a compromise such as the differentiator would be less sensible to the noise while preserving good convergence properties. This compromise gives $\theta^i = \frac{1}{2}$. However, it is interesting to have a better way to tune this parameter. In the sequel, parameter θ^i is dynamically adapted in order to take into account the presence (or not) of noisy measurement.

B. Case 2: time varying θ^i

As introduced just above, in order to improve the robustness toward the noise rejection, an adaptive scheme that drives the parameters θ^a and θ^b according to the maximum magnitude of the high frequency noise extracted from the signals y_a and y_b, is inspired from [13]. Depicted in Fig. 3, for both differentiation stages, the scheme is composed of a high pass filter (Butterworth of fourth order) that extracts the magnitude of the high frequency noise, denoted y_{HP}, for which the absolute magnitude is averaged through a low pass filter (with time-constant τ) and the variable θ^i is calculated from this averaged value:

$$\begin{cases} r_{k+1}^i = (1 + h\dfrac{1}{\tau}) r_k^i + \dfrac{1}{\tau} h |r_{HP}^i| \\ \\ \theta^i = g^i \dfrac{r^i}{r^i + \varepsilon^i} \end{cases} \tag{10}$$

where $g^i > 0$, τ^i and $\varepsilon^i > 0$ for $i \in \{a, b\}$ are respectively the output gains, the time-constants of the LP filters and scaling factors that manage the range of θ^i according to the "level" of $|y_{HP}|$.

General idea. The idea is the following: if high frequency noise level on the signal[1] y_a is very limited, then the signals y_{HF}^a and r^a tend to 0 that makes θ^a tending towards 0. The

[1]A similar reasoning can be made for y_b

projector (9) is then "tending" to (8): the convergence of the differentiator is achieved in a finite time. In the opposite case, *i.e.* y_a is noisy, then, y^a_{HF} and r^a are not equal to 0. Then, θ_a depends on the values of g^a, r^a and ε^a. From the knowledge of high frequency noise level on the measurement, r^a can be *a priori* evaluated that gives a way for the tuning of ε^a and g^a in order to keep $\theta^a < 1$. Then, the projector (9) has a reduced noise sensibility.

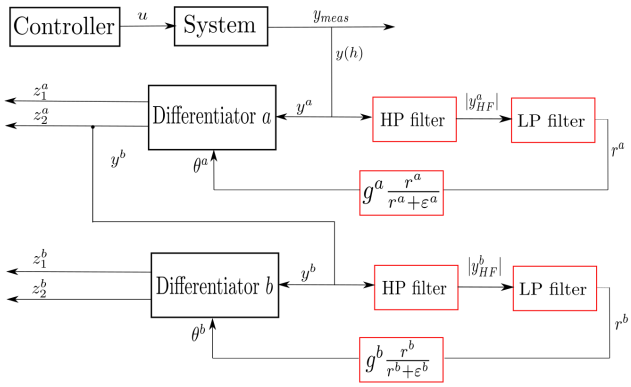

Fig. 3: Synoptic view of the proposed cascaded differentiators to estimate velocity and acceleration including the θ^i adaptive scheme.

These parameters, g^i, τ^i and ε^i, are adjusted by the user with respect to the quality of the measurement y_{meas}; an optimization procedure can also be used to adjust these parameters in order to improve the performances index [23]. The SSE index, which are evaluated by the optimization algorithm compared to the velocity and acceleration references, are minimized over the steady-state of each differentiator.

V. Experimental results

The following working hypotheses are made regarding the controlled trajectory and the choice of the sampling periods. The control of the position (not detailed here) is supposed to be efficient, and ensures a very accurate tracking of the reference trajectory. As a consequence, in the sequel, the estimated values will be compared with the desired trajectories. Remark that all the results provided by the proposed differentiators under study are not used in the control feedback.

A. Assumptions

The experimentations have been made in the following conditions.

- *Position reference.* The desired position reference is $y_{ref} = 0.04\sin(0.15t)$ and the control ensures a good tracking of the position (see. Fig. 4);
- *Velocity reference* The estimated velocity z_2 is compared to the derivative $\dot{y}_{ref}$;
- *acceleration reference* The estimated acceleration z_3 is compared to the second derivative $\ddot{y}_{ref}$;
- the sampling time of the differentiation is chosen in order to observe the effects of a possible under-sampling: the sampling time is set to 0.2 s.

The gains and parameters for each stage of the cascade are set as follows. The parameters λ_1, λ_2 and θ^i are chosen as follows: $\lambda_1 = \lambda_1^{'}\mu^{0.5}$ and $\lambda_2 = \lambda_2^{'}\mu$ as classically, where $\lambda_1^{'}$ and $\lambda_2^{'}$ ensure a pole-placement and μ is chosen greater than the maximum of the perturbation. This choice of gains is made to get acceptable performances [12] and one sets $\lambda^a_1 = \lambda^b_1 = 1.5$, $\lambda^a_2 = \lambda^b_2 = 0.625$, $\alpha_a = 0.75$, $\alpha_b = 0.7$.
Concerning the parameters θ_a and θ_b, one has

- Case 1 - constant θ^i: $\theta^a = \theta^b = 0.5$.
- Case 2 - varying θ^i: $\varepsilon^a = \varepsilon^b = 10^{-3}$, $g^a = 2.44$, and $g^b = 2.6$. The HP filters are Butterworth ones of 4^{th} order with a cut frequency of 1 Hz; the LP filters are first order ones with unitary gain and constant times $\tau^a = \tau^b = 0.2$ sec.

Remark : An optimization procedure optimizing SSE index (see next section) set the parameters $\varepsilon^\bullet$ and $\tau^\bullet$ as $\varepsilon^{\{a,b\}} = 10^{-3}$ and $\tau^{\{a,b\}} = 0.2$ sec while the gains g^a and g^b are set to different values according to the magnitude of the high frequency noise.

B. Results analysis

Figure 4 shows the controlled position according to the reference. Figures 6 and 7 illustrate the performances of the cascaded differentiator with the θ^i-constant strategy (case 1) for which the benefits of the implicit strategy are emphasized at low sampling frequency (see [12]). Figures 8 and 9 illustrate the performances of the cascaded differentiator to estimate respectively the velocity and the acceleration with the θ^i adaptive scheme. The Sum of Square Error (SSE)[2] index of velocity and acceleration errors are displayed in Fig. 5 for both fixed/varying θ^i methods; the smallest the SSE index, the better the result. Figures 10, 11 and 12 show respectively the outputs of the Butterworth HP filter, the outputs of the LP filters (that averages the absolute value of the high frequency noise) and the variations of $\theta^{a/b}$ according to the time.
Globally, the performances are improved with a varying θ^i parameter. The θ^i parameter evolves according to the magnitude of the noise. As a consequence, θ^i increases and then is acting on the projector (9) if the magnitude of the noise is high (and thus the corresponding estimation becomes smooth regarding the noise). If there is no noise, θ^i is close to zero and the differentiators remain in the "standard" form (7). Concerning the evolution of θ^a and θ^b, the noise on the velocity is amplified due to the differentiation and thus, the "effort" on the differentiator "b" is higher than the "effort" on the differentiator "a"; it follows that globally $\theta^b > \theta^a$ and θ^b tends to θ^a in the steady-state.

VI. Conclusion

Based on the recent experiments that have been conducted to investigate the promising properties of the differentiation

[2]The SSE is given by $\text{SSE}(\bullet) = \frac{1}{n}\sum_{l=1}^{n} \bullet_l^2$ with n the data size.

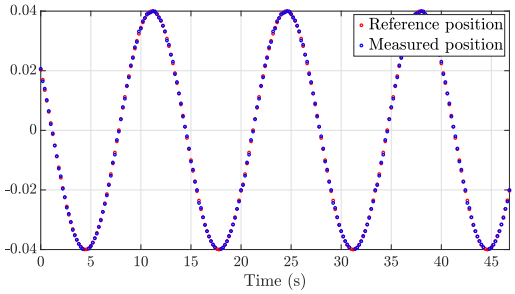

Fig. 4: Reference and measured position.

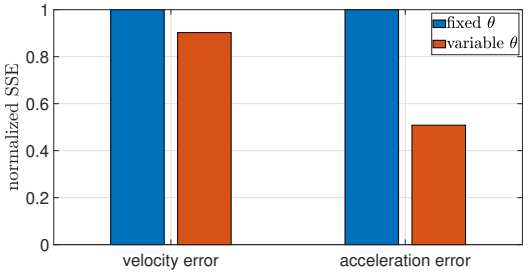

Fig. 5: Normalized SSE.

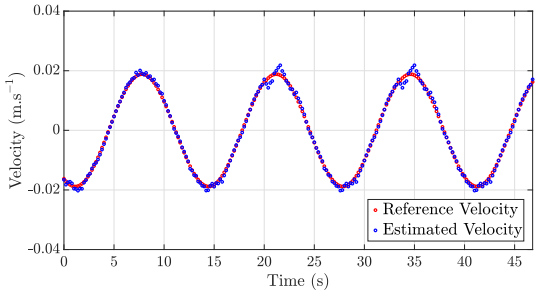

Fig. 6: Estimated velocity with θ^i constant versus time (s).

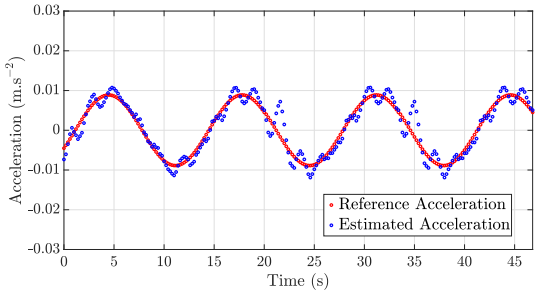

Fig. 7: Estimated acceleration with θ^i constant versus time (s).

methods within the Brogliato's & Acary's implicit framework, a cascaded-based structure of differentiation has been recently proposed and this work was dedicated to emphasize the noise rejection on the differentiation responses thanks to a new parameter θ^i included inside the implicit projector. An additional adaptive algorithm, based on the strategy developed in [13], drives θ^i according to the magnitude of the noise. The evaluation of the performances is made considering the velocity and acceleration estimation in presence of measurement noise thanks to a pneumatic setup for which the measured position has been differentiated twice using the proposed cascaded differentiation structure. As a result, the proposed θ^i adaptive structure highlights better performances in terms of the estimation precision and noise rejection. Future works include a complete study of the stability of this adaptive scheme within the semi-implicit framework as well as further experimental investigations to estimate velocity and acceleration in a robotics environment.

ACKNOWLEDGMENT

This work is supported by the ANR project DigitSlid ANR-18-CE40-0008-01.

REFERENCES

[1] V. Acary and B. Brogliato, "Implicit euler numerical scheme and chattering-free implementation of sliding mode systems," *Systems & Control Letters*, vol. 59, no. 5, pp. 284 – 293, 2010.

[2] O. Huber, V. Acary, and B. Brogliato, "Comparison between explicit and implicit discrete-time implementations of sliding-mode controllers," in *52nd IEEE Conf. on Decision and Control*, 2013, pp. 2870–2875.

[3] V. Acary, B. Brogliato, and Y. V. Orlov, "Chattering-free digital sliding-mode control with state observer and disturbance rejection," *IEEE Trans. on Automatic Control*, vol. 57, no. 5, pp. 1087–1101, 2012.

[4] O. Huber, V. Acary, B. Brogliato, and F. Plestan, "Discrete-time twisting controller without numerical chattering: analysis and experimental results with an implicit method," in *53rd IEEE Conf. on Decision and Control*, 2014, pp. 4373–4378.

[5] B. Wang, B. Brogliato, V. Acary, A. Boubakir, and F. Plestan, "Experimental comparisons between implicit and explicit implementations of discrete-time sliding mode controllers: Toward input and output chattering suppression," *IEEE Trans. on Control Systems Technology*, vol. 23, no. 5, pp. 2071–2075, 2015.

[6] B. Brogliato and A. Polyakov, "Globally stable implicit euler time-discretization of a nonlinear single-input sliding-mode control system," in *2015 54th IEEE Conf. on Decision and Control (CDC)*, 2015, pp. 5426–5431.

[7] O. Huber, V. Acary, and B. Brogliato, "Lyapunov stability and performance analysis of the implicit discrete sliding mode control," *IEEE Trans. on Automatic Control*, vol. 61, no. 10, pp. 3016–3030, 2016.

[8] B. Brogliato, A. Polyakov, and D. Efimov, "The implicit discretization of the super-twisting sliding-mode control algorithm," in *2018 15th International Workshop on Variable Structure Systems (VSS)*, 2018, pp. 349–353.

[9] ——, "The implicit discretization of the super-twisting sliding-mode control algorithm," *IEEE Trans. on Automatic Control*, pp. 1–1, 2019.

[10] A. Polyakov, D. Efimov, and B. Brogliato, "Consistent Discretization of Finite-time and Fixed-time Stable Systems," *SIAM Journal on Control and Optimization*, vol. 57, no. 1, pp. 78–103, 2019.

[11] L. Michel, M. Ghanes, F. Plestan, Y. Aoustin, and J. Barbot, "Semi-implicit euler discretization for homogeneous observer-based control: one dimensional case," in *Proc. of the IFAC-V 2020, World Congress*, Berlin, Germany, July 2020.

[12] L. Michel, S. Selvarajan, M. Ghanes, F. Plestan, Y. Aoustin, and J.-P. Barbot, *An experimental investigation of discretized homogeneous differentiators: pneumatic actuator case*. (in second lecture), 2020. [Online]. Available: https://box.ec-nantes.fr:443/index.php/s/A9T2cgBWJnxRns6/download

[13] M. Ghanes, J. P. Barbot, L. Fridman, A. Levant, and R. Boisliveau, "A new varying gain exponent based differentiator/observer: an efficient balance between linear and sliding-mode algorithms," *IEEE Trans. on Automatic Control*, 2020.

[14] A. Girin and F. Plestan, "A new experimental test bench for a

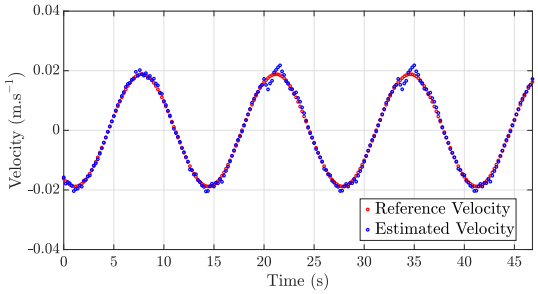

Fig. 8: Estimated velocity with θ^i variable versus time (s).

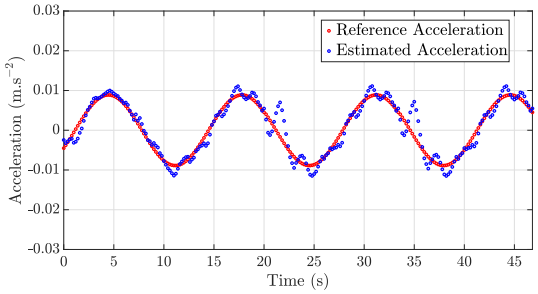

Fig. 9: Estimated acceleration with θ^i variable versus time (s).

high performance double electropneumatic actuator system," in *2009 American Control Conference*, 2009, pp. 3488–3493.

[15] E. Tahoumi, F. Plestan, M. Ghanes, and J. Barbot, "New robust control schemes based on both linear and sliding mode approaches: Design and application to an electropneumatic actuator," *IEEE Trans. on Control Systems Technology*, pp. 1–8, 2019.

[16] E. Tahoumi, F. Plestan, M. Ganes, and J. P. Barbot, "The implicit discretization of the super-twisting sliding-mode control algorithm," in *2018 European Control Conference*, 2018, pp. 2368–2373.

[17] W. Perruquetti and J. P. Barbot, *Sliding Mode Control in Engineering*. USA: Marcel Dekker, Inc., 2002.

[18] A. Polyakov, *Generalized Homogeneity in Systems and Control*. Springer Nature Switzerland AG: Springer-Verlag, 2020.

[19] A. Hanan, A. Jbara, and A. Levant, *New Homogeneous Controllers and Differentiators*. Cham: Springer International Publishing, 2020, pp. 3–28.

[20] C. Qian and W. Lin, "Recursive observer design, homogeneous approximation, and nonsmooth output feedback stabilization of nonlinear systems," *IEEE Trans. on Automatic Control*, vol. 51, no. 9, pp. 1457–1471, 2006.

[21] C. Qian and W. Lin, "Nonsmooth output feedback stabilization of a class of genuinely nonlinear systems in the plane," *IEEE Trans. on Automatic Control*, vol. 48, no. 10, pp. 1824–1829, 2003.

[22] B. Yang and W. Lin, "Output feedback stabilization of a class of homogeneous and high-order nonlinear systems," in *42nd IEEE Int. Conference on Decision and Control (IEEE Cat. No.03CH37475)*, vol. 1, 2003, pp. 37–42 Vol.1.

[23] M. Porcelli and P. L. Toint, "Bfo, a trainable derivative-free brute force optimizer for nonlinear bound-constrained optimization and equilibrium computations with continuous and discrete variables," *ACM Trans. Math. Softw.*, vol. 44, no. 1, Jun. 2017.

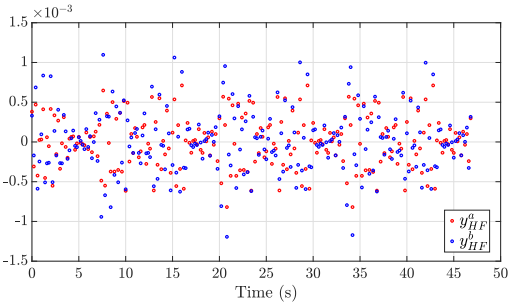

Fig. 10: HP filters outputs with θ^i adaptive versus time (s).

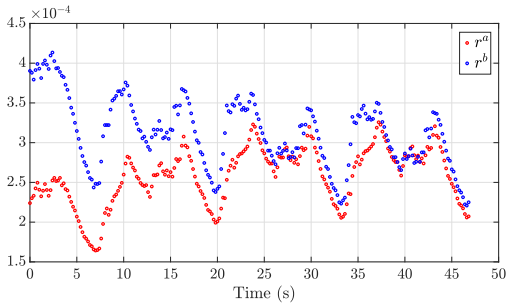

Fig. 11: LP filters outputs with θ^i adaptive versus time (s).

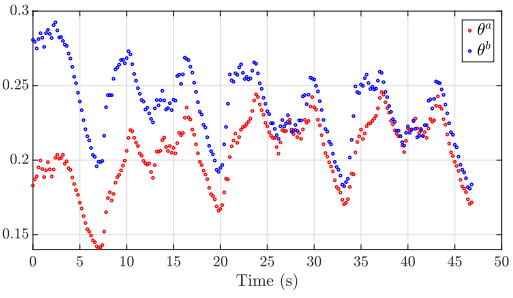

Fig. 12: θ^i variations with θ^i adaptive versus time (s).